

**X-ray absorption spectroscopy study of diluted magnetic  
semiconductors:**

**$Zn_{1-x}M_xSe$  (M = Mn, Fe, Co) and  $Zn_{1-x}Mn_xY$  (Y = Se, Te)**

Kwanghyun Cho, Hoon Koh, and S.-J. Oh\*

*Department of Physics & Center for Strongly Correlated Materials Research, Seoul National  
University, Seoul 151-742, Korea*

Hyeong-Do Kim and Moon-sup Han

*Department of Physics, University of Seoul, Seoul 130-743, Korea*

J.-H. Park

*Department of Physics, Pohang University of Science and Technology, Pohang 790-784, Korea*

C. T. Chen

*Synchrotron Radiation Research Center, Hsinchu Science-based Industrial Park, Hsinchu 300,  
Taiwan, Republic of China*

Y. D. Kim

*Department of Physics, Kyung Hee University, Seoul 130-701, Korea*

J.-S. Kim

*Department of Physics, Sook-Myung Women's University, Seoul 140-742, Korea*

B. T. Jonker

*Naval Research Laboratory, Washington, DC 20375-5343*

(Received )

## Abstract

We have investigated  $3d$  electronic states of doped transition metals in II-VI diluted magnetic semiconductors,  $\text{Zn}_{1-x}\text{M}_x\text{Se}$  ( $\text{M} = \text{Mn}, \text{Fe}, \text{Co}$ ) and  $\text{Zn}_{1-x}\text{Mn}_x\text{Y}$  ( $\text{Y} = \text{Se}, \text{Te}$ ), using the transition-metal  $L_{2,3}$ -edge X-ray absorption spectroscopy (XAS) measurements. In order to explain the XAS spectra, we employed a tetragonal cluster model calculation, which includes not only the full ionic multiplet structure but also configuration interaction (CI). The results show that CI is essential to describe the experimental spectra adequately, indicating the strong hybridization between the transition metal  $3d$  and the ligand  $p$  orbitals. In the study of  $\text{Zn}_{1-x}\text{Mn}_x\text{Y}$  ( $\text{Y} = \text{Se}, \text{Te}$ ), we also found considerable spectral change in the Mn  $L_{2,3}$ -edge XAS spectra for different ligands, confirming the importance of the hybridization effects in these materials.

PACS number(s): 71.23.An, 75.50.Pp, 78.70.Dm

## I. INTRODUCTION

There has been active studies on diluted magnetic semiconductors (DMS's) for the last two decades because of their unique magneto-optical and magneto-transport properties such as giant negative magnetoresistance, extremely large electronic  $g$  factor, large Faraday rotation, etc.<sup>1,2</sup> Recently the interest has surged again because of their possible applications to “spintronics” based on the semiconductor technology.<sup>3</sup> DMS's, which are made by substitution of small amount of late  $3d$  magnetic transition-metal (TM) atoms such as Mn, Fe, and Co ions into cation sites in the II-VI or III-V compound semiconductors, involve both semiconductor physics and magnetism. The band gap energy turns out to change with the doping concentration.<sup>7</sup> Moreover, in some DMS's, the variation of the doping concentration was found to induce magnetic phase transitions, such as paramagnetic to spin glass phase and spin glass to antiferromagnetic phase,<sup>1</sup> and even ferromagnetism can also be induced by injecting carriers or photon irradiation.<sup>8</sup>

Here our studies are mainly focused on the electronic structure of II-VI based DMS's. The II-VI compounds such as ZnSe and ZnTe have a zinc-blende crystal structure, in which the cation  $\text{Zn}^{2+}$  ions are under the tetrahedral  $T_d$  site symmetry. The TM doping induces merely small changes of the lattice-constants within the crystal structure. The  $(4sp)^2$  electrons of the TM atoms, which act like the Zn  $(4sp)^2$  electrons, participate in the ligand  $p$ -Zn  $4sp$  bonding-antibonding states. These states, which correspond to the respective valence band and conduction band of the host semiconductor, are hardly affected by the doping<sup>1,4</sup>. Meanwhile, the TM  $3d$  electrons provide rather localized additional band states, which is expected to be located energetically in the wide band gap of the bonding-antibonding states. Optical absorption studies of DMS's showed the intra-atomic  $d$ - $d$  transitions which can be understood by the  $3d$  Coulomb multiplets excited from the corresponding ionic high-spin ground state.<sup>5,6</sup> In spite of the ionic characteristics, the TM  $3d$  electrons are known to make strong covalent bonding with ligand  $p$  electrons. Furthermore, this covalent bonding, which is often represented by “ $p$ - $d$ ” hybridization, is expected to play an important role

in the interesting magneto-transport and magneto-optical properties such as giant Faraday rotation and Zeeman splitting.<sup>1</sup>

In order to understand the electronic structure of these DMS's, several photoemission spectroscopy measurements have been performed, mostly utilizing  $3p \rightarrow 3d$  resonance phenomena near the TM  $3p$  absorption edge.<sup>9,10</sup> This technique enables us to separate out the TM  $3d$  contribution to the electronic structure, and one can extract a sort of the  $3d$  partial spectral weight. The resulting  $3d$  spectral weight was found to be distributed in a very wide range of the valence band, no matter what the doping concentration is, indicating the strong  $p - d$  hybridization of ligand  $p$  band and the TM  $3d$  orbitals. Meanwhile, the  $3d$  spectral line shape does not agree with the band structure calculations.<sup>11,12</sup> For such reasons, the TM  $3d$  partial spectral weights have been tried to be interpreted in terms of a many-body approach like a cluster model calculation with configuration interaction<sup>5,10</sup> (CI) or an Anderson impurity model calculation.<sup>13</sup> These model calculations, which are characterized by phenomenological physical quantities such as TM  $3d$  on-site Coulomb energy,  $p - d$  hybridization, and the ligand  $p$  to TM  $3d$  charge transfer energy, have been very successful in describing the electronic structure of TM compounds.<sup>14</sup>

Soft x-ray absorption spectroscopy (XAS) is another powerful high-energy probe to investigate the electronic structure of transition metal compounds.<sup>15</sup> Especially in diluted systems, XAS has big advantages over the photoemission measurements. Figure 1 shows XAS spectra at TM  $L_{2,3}$ -edges of  $\text{Zn}_{1-x}\text{Mn}_x\text{Se}$  ( $x = 0.059$ ),  $\text{Zn}_{1-x}\text{Fe}_x\text{Se}$  ( $x = 0.049$ ), and  $\text{Zn}_{1-x}\text{Co}_x\text{Se}$  ( $x = 0.050$ ), which result from TM  $2p \rightarrow 3d$  dipole transitions. The spectra are dominated by the large  $2p$  core hole spin-orbit coupling energy, which divides them into roughly the  $L_3$  and  $L_2$  regions at low and high photon energy, respectively. The absorption process is a local process and its energy is determined by the characteristic core-hole energy. Despite the fact that the systems contain relatively small concentration of TM atoms, all the spectra nicely reveal the complex spectral structure, which is originated from the  $2p$  core-hole- $3d$  Coulomb multiplets, and one can determine important physical quantities to understand the electronic structure by analysing them.

The photoemission spectroscopy is known to directly probe the electronic structure and the TM  $3p$ -edge resonant photoemission spectroscopy enables us to extract the TM  $3d$  partial spectrum. However, the extracted spectrum somehow differs from the true TM  $3d$  electronic structure because of the different transition matrix elements in the resonant process from those in the direct photoemission process. Hence it is worthwhile to verify the physical quantities determined from the TM  $3p$ -edge resonant photoemission studies by analysing the XAS results. Furthermore, in a view of the experimental technique, the XAS is rather bulk-sensitive, different from the resonant photoemission spectroscopy, and the results are much less sensitive to the surface condition of samples. Only a few XAS studies, however, have been performed for DMS's so far.<sup>16–19</sup> Further, the reported studies were mostly focused on XAS spectra of the ligand atoms such as S  $K$ -edge<sup>17</sup> and Te  $L_1$ -edge and  $L_3$ -edge.<sup>18</sup> The studies concluded qualitatively that the  $p$ - $d$  hybridization is strong and the  $p$ - $d$  hybridization strength depends on the ligand ions.<sup>19</sup> However, quantitative analysis for the electronic structure has not been carried out.

In this paper, we report high-resolution XAS studies to investigate the electronic structure of various II-VI DMS's. The XAS spectra at the TM  $L_{2,3}$  edges are analysed by using a tetrahedral cluster model calculation including CI as well as the full ionic multiplets. Previously, the model calculations for TM  $L_{2,3}$ -edge XAS spectra were performed only for condensed systems such as divalent Ni compounds,<sup>20</sup>  $\text{Ti}_2\text{O}_3$ ,<sup>21</sup>  $\text{CoO}$ ,<sup>22</sup> and  $\text{LiVO}_2$ .<sup>23</sup>, and showed that the CI considerably affects the XAS spectrum. Thus it is also important to elucidate how the effects of CI appear in the XAS spectra of diluted systems like DMS's.

## II. EXPERIMENT

The samples used in this study were  $\text{Zn}_{1-x}\text{Mn}_x\text{Se}$  ( $x = 0.059$ ),  $\text{Zn}_{1-x}\text{Fe}_x\text{Se}$  ( $x = 0.049$ ), and  $\text{Zn}_{1-x}\text{Co}_x\text{Se}$  ( $x = 0.050$ ) thin films grown by molecular beam epitaxy on the GaAs (001) substrate and a  $\text{Zn}_{1-x}\text{Mn}_x\text{Te}$  ( $x = 0.60$ ) single crystal with (110) surface. The details of the sample growth and characterization were reported elsewhere.<sup>4</sup> All the samples preserve

the zinc-blende crystal structure. The XAS measurements were carried out at the Dragon high-resolution soft-x-ray beam line<sup>24</sup> at the National Synchrotron Light Source, Brookhaven National Laboratory. The energy resolution of incoming photon was set to be about 0.5 eV in the full width at half maximum (FWHM). Before the measurements, the single-crystalline sample was cleaved *in situ* and the thin-film samples, which had been pre-etched using 1:3 mixture of NH<sub>4</sub>OH (29 %):methanol,<sup>25</sup> were annealed *in situ* at 300 °C by radiation heating for about three hours.<sup>26</sup> The measurements were performed at room temperature and the base pressure was maintained below  $2 \times 10^{-10}$  Torr.

### III. CALCULATIONAL METHOD

A tetrahedral cluster model calculation, which we have employed to analyse the XAS spectra, includes not only the full multiplets of TM  $3d$  electrons but also configuration interaction. The model is characterized by the on-site  $3d$  Coulomb energy,  $U \equiv E(d^{n+1}) + E(d^{n-1}) - 2E(d^n)$ , the ligand-to- $3d$  charge-transfer energy,  $\Delta \equiv E(d^{n+1}\underline{L}) - E(d^n)$ , and the cation- $d$ -ligand- $p$  hybridization strength  $V$ . The initial configuration states are spanned over the ionic ground state  $3d^n$  and the charge-transferred states,  $3d^{n+1}\underline{L}, \dots, 3d^{10}\underline{L}^{10-n}$ , where  $\underline{L}$  denotes a ligand- $p$  hole. The multiplets of the  $3d$  electron configurations in the charge transferred states are taken into account explicitly while the total symmetry is preserved to be the same as the ionic ground state symmetry. The  $3d$  Coulomb exchange interactions are represented by Racah parameters,  $B$  and  $C$ . Although the Racah parameters can vary slightly in different configurations, we imported the values from Ref. 5 and fixed them in all configurations for the sake of simplicity. The on-site Coulomb  $U$  and the charge transfer energy  $\Delta$  are treated as control parameters in the calculation and defined with the lowest-energy  $3d$  multiplet states of the corresponding configurations.

Similarly, the final states are also spanned over  $\underline{2p}3d^{n+1}, \underline{2p}3d^{n+2}\underline{L}, \dots, \underline{2p}3d^{10}\underline{L}^{9-n}$  configuration states. The Coulomb energies between the  $2p$  core-hole and a  $3d$  electron are represented by the  $2p$ - $3d$  Slater integrals,  $F_{pd}^2$ ,  $G_{pd}^1$ , and  $G_{pd}^3$ , and the spin-orbit coupling of

the  $2p$  core-hole is taken into account with ( $\zeta_{2p}$ ). The involved parameter values are borrowed from Ref. 28 and fixed for all configurations. The Slater integrals were scaled down by a reduction factor  $\kappa$  in order to account for the solid state screenings.<sup>29</sup> The average Coulomb interaction  $Q$  between a TM  $2p$  hole and a  $3d$  electron is set to be an empirical value of  $1.25U$  as widely adopted in the core-level spectroscopy studies.

The hybridization interactions are expressed in terms of the Slater-Koster parameters  $V_{pd\sigma}$  and  $V_{pd\pi}$ :  $V_t \equiv \langle t|H|L_t \rangle = \sqrt{\frac{4}{3}V_{pd\sigma}^2 + \frac{8}{9}V_{pd\pi}^2}$  and  $V_e \equiv \langle |H|L_e \rangle = \frac{2\sqrt{6}}{3}V_{pd\pi}$ , where  $t(e)$  and  $L_t$  ( $L_e$ ) are TM- $3d$  and ligand- $p$  orbitals with  $t_{2g}$  ( $e_g$ ) symmetry orbitals under  $T_d$  tetrahedral point group symmetry, respectively. For simplicity, we apply the empirical relation  $V_{pd\sigma} = -2V_{pd\pi}$ .<sup>30</sup> The crystal-field interaction  $10Dq$  is fixed to be 0.25 eV in all the calculations, and the reason will be explained later. Here TM  $3d$  spin-orbit coupling is neglected. It is known that the  $3d$  spin-orbit coupling can be quenched when the ground-state orbital symmetry is either  $A$  or  $E^{28}$ , and indeed, the ground state symmetries of  $\text{Mn}^{2+}$ ,  $\text{Fe}^{2+}$ , and  $\text{Co}^{2+}$  ions are  ${}^6A_1$ ,  ${}^5E$ , and  ${}^4A_2$  under the  $T_d$  symmetry, respectively.

The initial ground state is obtained in the modified Lanczos method. Then the XAS spectra are calculated by the continued fraction expansion.<sup>31</sup> The calculated spectrum is broadened with a Lorentzian function, which accounts for the core-hole lifetime, and finally with a Gaussian function for the experimental resolution (0.5 eV). The Lorentzian broadenings,  $\Gamma_2$  for  $L_2$ -edge and  $\Gamma_3$  for  $L_3$ -edge spectra are presented in Table I.

## IV. RESULTS AND DISCUSSION

### A. CI effects on the cluster model calculation

The calculated TM  $L_{2,3}$ -edge XAS spectra for  $\text{Mn}^{2+}$ ,  $\text{Fe}^{2+}$ , and  $\text{Co}^{2+}$  ions, which are in a tetrahedral cluster, are presented in Figure 2 in comparison with the corresponding experimental XAS spectra of  $\text{Zn}_{1-x}\text{Mn}_x\text{Se}$  ( $x = 0.059$ ),  $\text{Zn}_{1-x}\text{Fe}_x\text{Se}$  ( $x = 0.049$ ), and  $\text{Zn}_{1-x}\text{Co}_x\text{Se}$  ( $x = 0.050$ ), respectively. Now the photon energy is presented relative to that of the corre-

sponding main  $L_3$  multiplet peak with the highest intensity. In order to investigate the role of configuration interaction, the calculation has been performed for the orders of the charge transferred states.

In the zero-th order calculations, which are denoted by  $\underline{L}^0$ , the charge transferred states are neglected, *i.e.* the ionic calculations. Meanwhile in the  $m$ -th order calculations, denoted by  $\underline{L}^m$ , the charge transferred states are included up to the configuration states with  $m$  ligand holes, *i.e.* the calculations with the configuration states of  $3d^n$ ,  $3d^{n+1}\underline{L}^1$ ,  $\dots$ ,  $3d^{n+m}\underline{L}^m$  for the initial states and the configuration states of  $\underline{2p}3d^{n+1}$ ,  $\underline{2p}3d^{n+2}\underline{L}^1$ ,  $\dots$ ,  $\underline{2p}3d^{n+m+1}\underline{L}^m$  for the final states. The spectra are normalized by the intensity of the  $L_3$  main peak. For a given TM ion, the same parameter set is employed for the  $\underline{L}^0$ ,  $\dots$ , the  $\underline{L}^m$  calculations.

When we take into account only the  $\underline{L}^1$  charge transferred states, we find that the calculated spectrum changes considerably from the  $\underline{L}^0$  spectra, especially in the cases of  $\text{Fe}^{2+}$  and  $\text{Co}^{2+}$  ions.<sup>32</sup> But the  $\underline{L}^2$  spectra are nearly the same as the  $\underline{L}^1$  spectra, indicating that the CI effects on the spectrum converge very rapidly. It is because the energies of the  $3d^{n+2}\underline{L}^2$  and  $\underline{2p}3d^{n+3}\underline{L}^2$  configuration states already become much higher than those of  $3d^{n+1}\underline{L}^1$  and the  $\underline{2p}3d^{n+2}\underline{L}^1$  states, due to the strong on-site Coulomb interaction. Thus we will consider, from now on, only the result of calculations which include configurations up to  $d^{n+2}\underline{L}^2$  and  $\underline{p}d^{n+3}\underline{L}^2$ . Here the parameter values are chosen to give the  $\underline{L}^2$  spectra, which agree well with the corresponding experimental ones.

As can be seen in Fig. 2, the spectrum is strongly disturbed by CI, especially in high energy region of the main  $L_3$  multiplet peak. The peak separation becomes reduced and the sharp peak structure is smeared out with CI. Although similar trend might be reproduced just by increasing the crystal field splitting  $10Dq$  value without including CI,<sup>28</sup> we believe CI is essential for proper interpretation of the XAS spectra for the following reason. When we increase the value of  $10Dq$  without including CI, the pre-edge structure is well separated from the main peak and grows rapidly. At the same time the  $L_2$ -edge spectrum becomes very complicated except for a  $\text{Co}^{2+}$  ion,<sup>33</sup> neither of which is observed in the experimental spectra. Hence,  $10Dq$  value should be small for  $\text{Mn}^{2+}$  and  $\text{Fe}^{2+}$  ions but large for a  $\text{Co}^{2+}$

ion if one fits the experimental spectra without CI. It is, however, hard to believe that the  $10Dq$  value, which reflects the hybridization strength in the calculation, changes abruptly along this series.<sup>34</sup>

In the comparison of the calculated spectra with the experimental ones, the agreement is rather good in overall. But one can still recognize some minor disagreement, which is expected to arise from the uncertainties in Slater integrals and spin-orbit coupling parameters and the solid state effects which have been left out in the cluster model. Each final state multiplet may have different lifetime, and thus for the better fit, one should apply an appropriate core-hole-lifetime broadening for each multiplet state. The solid state effects seem to be rather severe in the spectrum of a  $\text{Co}^{2+}$  ion, and thus we employed the reduction factor  $\kappa$  smaller than other TM ions.

The parameter values for the best fit are tabulated in Table 1. The ligand-to- $3d$  charge transfer energy  $\Delta$  of Mn, Fe, and Co DMS's are 5.0, 3.0, and 2.5 eV, respectively. Here  $\Delta$  is defined with respect to the center of the multiplet. The decreasing behavior of  $\Delta$  value along the series agrees with the decrease of the difference in the electro-negativity between TM and ligand atoms. These values are similar to them obtained from the  $d-d$  optical-absorption study.<sup>5</sup> The hybridization parameter  $V_{pd\sigma}$  are determined to be 1.0, 0.9, and 0.8 eV for Mn, Fe, and Co DMS's, respectively. The small decrease of  $V_{pd\sigma}$  with the increasing atomic number is also consistent with the expected contraction of the  $3d$  electron wave function, but these values are somewhat smaller than those obtained from the analysis of photoemission spectra.<sup>5,10</sup> This is probably due to the small reduction of the effective hybridization strength in the XAS final states induced by the strong Coulomb potential by the localized core orbitals as pointed by Gunnarsson and Jepsen.<sup>35</sup> Similar behavior is also observed in the analysis of the Ni compounds using the Anderson impurity model.<sup>20</sup>

## B. Hybridization effect

In order to study the details of the hybridization effect, we compared the XAS spectra of  $\text{Zn}_{1-x}\text{Mn}_x\text{Se}$  and  $\text{Zn}_{1-x}\text{Mn}_x\text{Te}$  where different ligands will give variations in the charge-transfer energy  $\Delta$  and the hybridization interaction  $V_{pd\sigma}$ . As can be seen in Fig. 1, the Mn  $L_3$ -edge XAS spectrum shows a simple and distinguishable multiplet structure, and thus is very appropriate to study the variation of the hybridization effect. Figure 3 shows the experimental XAS spectra of  $\text{Zn}_{0.941}\text{Mn}_{0.059}\text{Se}$  and  $\text{Zn}_{0.4}\text{Mn}_{0.6}\text{Te}$  at the Mn  $L_3$ -edge together with the corresponding calculated ones.<sup>27</sup> The experimental spectra show four peak structure, a highest intensity peak (denoted by  $A$ ), two high energy peaks at about 1 eV (denoted by  $B$ ) and 3.5 eV (denoted by  $C$ ) above, and a small pre-edge structure (denoted by  $D$ ), for both compounds. This structure is mainly originated from the Mn  $2p^53d^6$  XAS final state multiplets of the  $\text{Mn}^{2+}$  ion.

The spectra display the common multiplet structure, but one can still recognize considerable difference in the relative peak energies and intensities for different ligand-ions. For examples, the relative energy of the peak B is lower for Te-ligand ions, while the width of the peak C is narrower for the Se-ligand ions. The best fits for the multiplet of these two compounds were obtained with the parameter values of  $\Delta = 5.0$  eV and  $V_{pd\sigma} = 1.00$  eV for  $\text{Zn}_{0.941}\text{Mn}_{0.059}\text{Se}$  and  $\Delta = 3.8$  eV and  $V_{pd\sigma} = 0.90$  eV for  $\text{Zn}_{0.4}\text{Mn}_{0.6}\text{Te}$ . Other parameters such as the on-site Coulomb interaction  $U$  and the crystal-field interaction  $10Dq$  are fixed to be 8.0 eV and 0.25 eV, respectively, since they are expected to be hardly affected by the variation of the ligand ions. In the picture,  $\Delta$  and  $V_{pd\sigma}$  mainly determine the hybridization strength between TM- $d$  and ligand- $p$  orbitals.

As can be seen in the figure, the calculated spectra show good over all agreement with the experimental ones. Chemical trends of the parameter values are consistent with the electro-negativity of ligand ions and also with the nearest neighbor distances between Mn and ligand ions. According to the Harrison's scheme,<sup>30</sup> the bond-length ( $d$ ) dependence of  $V_{pd\sigma}$  is  $d^{-3.5}$ , but the obtained values yield  $d^{-1.4}$  dependence using a simple central-force

model<sup>36</sup> for the Mn-anion bond length. Such a disagreement, which was also observed by Larson *et al.*, may be attributed to the chemical difference between Te and Se ions.<sup>12</sup> The agreement in the region of the second satellite is not as good as the first satellite, especially in  $\text{Zn}_{0.4}\text{Mn}_{0.6}\text{Te}$ . We suspect that this is probably due to the magnetic interaction between  $\text{Mn}^{2+}$  ions in this Mn-rich compound, which can affect the spectral shape considerably.<sup>37</sup>

It is worthwhile to understand how the XAS spectrum is affected by the parameters  $\Delta$  and  $V_{pd\sigma}$ . Fig. 4 shows the XAS spectra as a function of  $\Delta$  for a fixed  $V_{pd\sigma} = 1.0$  eV in the left panel and the spectra as a function of  $V_{pd\sigma}$  for a fixed  $\Delta = 4.0$  eV in the right panel. First, the calculation results show that the position of the peak *B* is closer to the peak *A* and its intensity becomes smaller when the hybridization effect increases by decrease of  $\Delta$  or increase of  $V_{pd\sigma}$ . Second, the structure *C* in the experimental spectrum seems to be a single peak structure. However, it turns out to consist of several multiplet states. Third, the pre-edge structure *D* is mainly induced by the crystal-field splitting  $10Dq$ . This structure is absent at  $10Dq = 0$  but becomes distinguishable for large  $10Dq$ -value.<sup>28</sup> In our parameter set with small  $10Dq$ , the structure *D* is barely recognized as in the experimental results. In practice, it is difficult to determine the exact value of  $10Dq$  from the fitting of XAS spectra, and we simply fixed  $10Dq = 0.25$  eV just enough to show the structure *D*.

## V. CONCLUSION

XAS spectra of various DMS's at the TM atom  $L_{2,3}$  edges are presented and described by a tetrahedral cluster model including full multiplet structure and configuration interaction. Due to the strong hybridization between the TM- $3d$  and ligand- $p$  orbitals, inclusion of CI with reasonable physical parameters gives much better results than the model without CI. Thus it is important to incorporate CI for understanding of the XAS spectra of DMS's. Hybridization effects on XAS spectra are also investigated varying ligand ions of Mn DMS's, and the change of the spectral shape is well explained by the cluster model with CI.

## ACKNOWLEDGMENTS

This work was supported by the Korean Science and Engineering Foundation (KOSEF) through the Center for Strongly Correlated Materials Research (CSCMR) at Seoul National University (2000), and Grant No. KOSEF 951-0209-014-1. J.-S. Kim acknowledges the support from Atomic Scale Surface Science Research Center (ASSRC) at Yonsei University. The work is also supported by BK21 project of Ministry of Education, Korea (SNU, POSTECH, and Kyung Hee U.). National Synchrotron Light Source, Brookhaven National Laboratory, at which the XAS data were obtained, is supported by the US Department of Energy. We also thank Prof. M. Taniguchi of Hiroshima University, Japan, for providing a  $\text{Zn}_{0.4}\text{Mn}_{0.6}\text{Te}$  single crystal.

## REFERENCES

\* Author to whom all correspondence should be addressed.

<sup>1</sup> J. K. Furdyna, *J. Appl. Phys.* **53**, 7637 (1982); *ibid.* **64**, R29 (1988).

<sup>2</sup> *Diluted Magnetic Semiconductors, Semiconductors and Semimetals* Vol. 25, edited by J. K. Furdyna and J. Kossut (Academic, New York, 1988); *Diluted Magnetic Semiconductors*, edited by M. Jain (World Scientific, Singapore, 1991).

<sup>3</sup> R. Fiederling, M. Keim, G. Reuscher, W. Ossau, G. Schmidt, A. Waag, and L. W. Molenkamp, *Nature (London)* **402**, 787 (1999); Y. Ohno, D. K. Young, B. Beschoten, F. Matsukura, H. Ohno, and D. D. Awschalom, *ibid.* **402**, 790 (1999); T. Dietl, H. Ohno, F. Matsukura, J. Cibert, and D. Ferrand, *Science* **287**, 1019 (2000).

<sup>4</sup> B. T. Jonker, J. J. Krebs, G. A. Prinz, X. Liu, A. Petrou, and L. Salamanca-Young, in *Growth, Characterization and Properties of Ultrathin Magnetic Films and Multilayers*, edited by B. T. Jonker, J. P. Heremans, and E. E. Marinero, MRS Symposia Proceedings No. 151 (Materials Research Society, Pittsburgh, 1989), p. 151, and references therein.

<sup>5</sup> T. Mizokawa and A. Fujimori, *Phys. Rev. B* **48**, 14 150 (1993).

<sup>6</sup> J. M. Noras, H. R. Szawelska, and J. W. Allen, *J. Phys. C: Solid State Phys.* **14**, 3255 (1981); C. Chen, X. Wang, Z. Qin, W. Wu, and W. Giriat, *Solid State Commun.* **87**, 717 (1993).

<sup>7</sup> Y. D. Kim, S. L. Cooper, M. V. Klein, and B. T. Jonker, *Phys. Rev. B* **49**, 1732 (1994).

<sup>8</sup> H. Ohno, A. Shen, F. Matsukura, A. Oiwa, A. Endo, S. Katsumoto, and Y. Iye, *Appl. Phys. Lett.* **69**, 363 (1996); S. Koshihara, A. Oiwa, M. Hirasawa, S. Katsumoto, Y. Iye, C. Urano, H. Takagi, and H. Munekata, *Phys. Rev. Lett.* **78**, 4617 (1997).

<sup>9</sup> A. Franciosi, C. Caprile, and R. Reifenberger, *Phys. Rev. B* **31**, 8061 (1985); M. Taniguchi, L. Ley, R. L. Johnson, J. Ghijsen, and M. Cardona, *ibid.* **33**, 1206 (1986); A. Wall, A.

- Franciosi, D. W. Niles, R. Reifenberger, C. Quaresima, M. Capozzi, and P. Perfetti, *ibid.* **41**, 5969 (1990); A. Wall, A. Raisanen, G. Haugstad, L. Vanzetti, and A. Franciosi, *ibid.* **44**, 8185 (1991); R. Weidemann, H.-E. Gumlich, M. Kupsch, H.-U. Middelmann, and U. Becker, *ibid.* **45**, 1172 (1992); N. Happo, H. Sato, K. Kimura, S. Hosokawa, M. Taniguchi, Y. Ueda, and M. Koyama, *ibid.* **50**, 12 211 (1994).
- <sup>10</sup> L. Ley, M. Taniguchi, J. Ghijsen, R. L. Johnson, and A. Fujimori, Phys. Rev. B **35**, 2839 (1987); M. Taniguchi, M. Fujimori, M. Fujisawa, T. Mori, I. Souma, and Y. Oka, Solid State Commun. **62**, 431 (1987); R. Denecke, L. Ley, and J. Fraxedas, Phys. Rev. B **47**, 13 197 (1993); Y. Ueda, M. Taniguchi, T. Mizokawa, A. Fujimori, I. Souma, and Y. Oka, *ibid.* **49**, 2167 (1994).
- <sup>11</sup> S.-H. Wei and A. Zunger, Phys. Rev. B **35**, 2340 (1987).
- <sup>12</sup> B. E. Larson, K. C. Haas, H. Ehrenreich, and A. E. Carlsson, Phys. Rev. B **37**, 4137 (1988).
- <sup>13</sup> O. Gunnarsson, O. K. Andersen, O. Jepsen, and J. Zaanen, Phys. Rev. B **39**, 1708 (1989).
- <sup>14</sup> A. Fujimori and F. Minami, Phys. Rev. B **30**, 957 (1984); J. Zaanen, G. A. Sawatzky, and J. W. Allen, Phys. Rev. Lett. **55**, 418 (1985).
- <sup>15</sup> *Photoemission and Absorption Spectroscopy of Solids and Interfaces with Synchrotron Radiation*, edited by M. Campagna and R. Rosei (North-Holland, Amsterdam, 1990).
- <sup>16</sup> A. Kisiel, A.-I. Ali Dahr, P. M. Lee, G. Dalba, P. Fornasini, and E. Burattini, Phys. Rev. B **44**, 11075 (1991).
- <sup>17</sup> W. F. Pong, R. A. Mayanovic, K. T. Wu, P. K. Tseng, B. A. Bunker, A. Hiraya, and M. Watanabe, Phys. Rev. B **50**, 7371(1994); K. Ławniczak-Jablonska, R. J. Iwanowski, Z. Gołacki, A. Traverse, S. Pizzini, A. Fontaine, I. Winter, and J. Hormes, *ibid.* **53**, 1119 (1996); K. Ławniczak-Jablonska, R. C. C. Perera, J. H. Underwood, E. M. Gullikson, and R. J. Iwanowski, *ibid.* **55**, 10 376 (1997).

- <sup>18</sup> J. Oleszkiewicz, M. Podgórnny, A. Kisiel, and E. Burattini, Phys. Rev. B **60**, 4920 (1999).
- <sup>19</sup> W. F. Pong, R. A. Mayanovic, J. K. Kao, H. H. Hsieh, J. Y. Pieh, Y. K. Chang, K. C. Kuo, P. K. Tseng, and J. F. Lee, Phys. Rev. B **55**, 7633 (1997).
- <sup>20</sup> G. van der Laan, J. Zaanen, G. A. Sawatzky, R. Karnatak, and J.-M. Esteve, Phys. Rev. B **33**, 4253 (1986).
- <sup>21</sup> T. Uozumi, K. Okada, A. Kotani, Y. Tezuka, and S. Shin, J. Phys. Soc. Jpn. **65**, 1150 (1996).
- <sup>22</sup> K. Okada and A. Kotani, J. Phys. Soc. Jpn. **61**, 449 (1992).
- <sup>23</sup> H. F. Pen, L. H. Tjeng, E. Pellegrin, F. M. F. de Groot, G. A. Sawatzky, M. A. van Veenendaal, and C. T. Chen, Phys. Rev. B **55**, 15500 (1997).
- <sup>24</sup> C. T. Chen and F. Sette, Rev. Sci. Instrum. **60**, 1616 (1989).
- <sup>25</sup> Y.-D. Kim, S. L. Cooper, M. V. Klein, and B. T. Jonker, Appl. Phys. Lett. **62**, 2387 (1993).
- <sup>26</sup> K. M. Colbow, Y. Gao, T. Tiedje, J. R. Dahn, and W. Eberhart, J. Vac. Sci. Technol. **A** **9**, 2614 (1991).
- <sup>27</sup> We could not find any noticeable difference in the Mn  $L_{2,3}$ -edge XAS spectrum for different  $x$  in  $Zn_{1-x}Mn_xSe$  ( $x=0.059, 0.1$ ).
- <sup>28</sup> G. van der Laan and I. W. Kirkman, J. Phys.: Condens. Matter **4**, 4189 (1992).
- <sup>29</sup> D. W. Lynch and R. D. Cowan, Phys. Rev. B **36**, 9228 (1987).
- <sup>30</sup> W. A. Harrison, *Electronic Structure and the Properties of Solids* (W. H. Freeman & Co., San Francisco, 1980).
- <sup>31</sup> E. R. Gagliano, E. Dagotto, A. Moreo, and F. C. Alcaraz, Phys. Rev. B **34**, 1677 (1986); E. Dagotto, R. Joynt, A. Moreo, S. Bacci, and E. Gagliano, *ibid.* **41**, 9049 (1990).

- <sup>32</sup> For a  $\text{Mn}^{2+}$  ion, the effect is still noticeable but small. The reason might be that the  $\text{Mn}^{2+}$  ion has relatively simple multiplet structure in comparison with other ions.
- <sup>33</sup> F. M. F. de Groot, M. Grioni, J. C. Fuggle, J. Ghijsen, G. A. Sawatzky, H. Petersen, Phys. Rev. B **40**, 5715 (1989).
- <sup>34</sup> J. Park, S. Ryu, M.-s. Han, and S.-J. Oh, Phys. Rev. B **37**, 10867 (1988).
- <sup>35</sup> O. Gunnarsson and O. Jepsen, Phys. Rev. B **38**, 3568 (1988).
- <sup>36</sup> C. K. Shih, W. E. Spicer, W. A. Harrison, and A. Sher, Phys. Rev. B **31**, 1139 (1985).
- <sup>37</sup> M. A. van Veenendaal, D. Alders, and G. A. Sawatzky, Phys. Rev. B **51**, 13 966 (1995).

## TABLES

TABLE I. Parameters used to calculate TM  $L_{2,3}$ XAS spectra of  $\text{Zn}_{1-x}\text{Mn}_x\text{Se}$  ( $x = 0.059$ ),  $\text{Zn}_{1-x}\text{Fe}_x\text{Se}$  ( $x = 0.049$ ), and  $\text{Zn}_{1-x}\text{Co}_x\text{Se}$  ( $x = 0.050$ ). See text for detailed explanations. All the values are given in eV.

	$\Delta$	$V_{pd\sigma}$	$U$	$Q$	$B$	$C$	$F_{pd}^2$	$G_{pd}^1$	$G_{pd}^3$	$\zeta_{2p}$	$\kappa$	$\Gamma_2$	$\Gamma_3$
$\text{Mn}^{2+}$	5.0	1.00	8.0	10.0	0.119	0.412	6.321	4.606	2.618	6.846	0.8	0.45	0.35
$\text{Fe}^{2+}$	3.0	0.90	3.6	4.5	0.131	0.484	6.793	5.004	2.844	8.200	0.8	0.70	0.45
$\text{Co}^{2+}$	2.5	0.80	4.8	6.0	0.138	0.541	7.259	5.397	3.069	9.748	0.7	1.00	0.50

## FIGURES

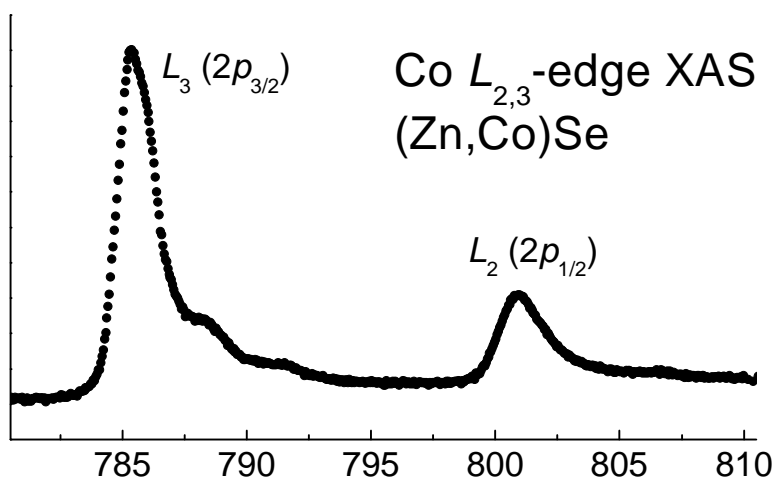
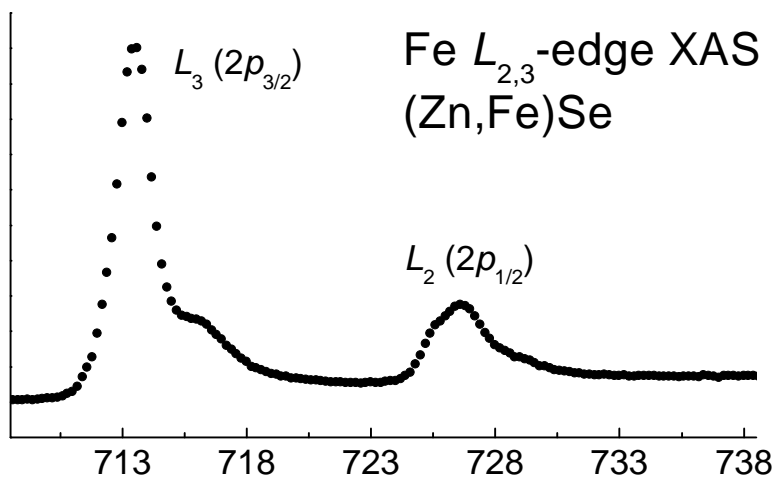
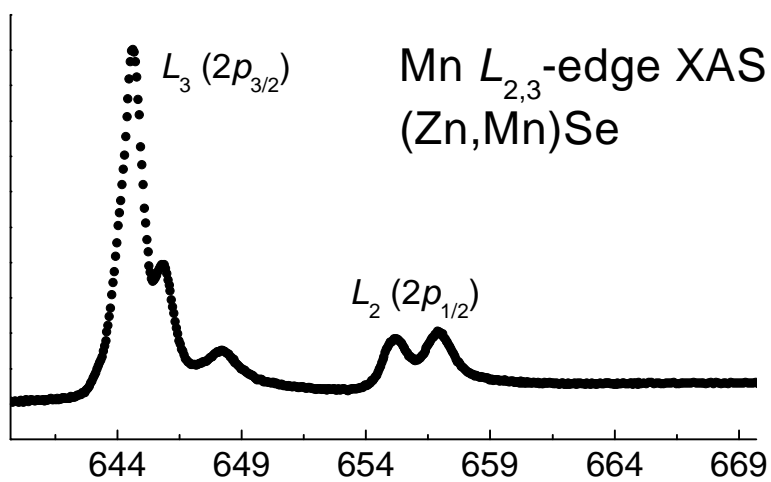
FIG. 1. Experimental XAS spectra of  $\text{Zn}_{1-x}\text{Mn}_x\text{Se}$  ( $x = 0.059$ ),  $\text{Zn}_{1-x}\text{Fe}_x\text{Se}$  ( $x = 0.049$ ), and  $\text{Zn}_{1-x}\text{Co}_x\text{Se}$  ( $x = 0.050$ ) at the TM  $L_{2,3}$  edges.

FIG. 2. Experimental (dots) and Calculated (lines)  $L_{2,3}$  XAS spectra of  $\text{Mn}^{2+}$ ,  $\text{Fe}^{2+}$ , and  $\text{Co}^{2+}$  ions in a tetrahedral cluster depending on the number of configurations employed.  $\underline{L}^n$  denotes a configuration, which contains a  $\underline{L}^n$  term in the initial and final states, up to which was included in the calculations. See text for detailed information on employed parameter values.

FIG. 3. Experimental (dots) and calculated (lines) XAS spectra of  $\text{Zn}_{1-x}\text{Mn}_x\text{Se}$  ( $x = 0.059$ ) and  $\text{Zn}_{1-x}\text{Mn}_x\text{Te}$  ( $x = 0.60$ ) at the Mn  $L_3$  edge. The vertical line is a guide for the peak position. For parameter values of the calculations, refer to text.

FIG. 4. Calculated  $L_3$  XAS spectra of a  $\text{Mn}^{2+}$  ion in a tetrahedral cluster. Left panel: As a function of  $\Delta$ .  $V_{pd\sigma}$  is fixed to 1.0 eV. Right panel: As a function of  $V_{pd\sigma}$ .  $\Delta$  is fixed to 4.0 eV. The vertical line is a guide for the peak position.

Intensity (arb. units)



Photon energy (eV)

